Materials & Design 212 (2021) 110188

Contents lists available at ScienceDirect

Materials & Design

journal homepage: www.elsevier.com/locate/matdes

Ni-Fe layered double hydroxides for oxygen evolution Reaction: Impact of Ni/Fe ratio and crystallinity

Manon Wilhelm [a], Alexandre Bastos [a], Cristina Neves [a], Roberto Martins [b], João Tedim [a,*]

[a] CICECO-Aveiro Institute of Materials, Department of Materials and Ceramic Engineering, University of Aveiro, 3810-193 Aveiro, Portugal
[b] CESAM- Centre for Environmental and Marine Studies, Department of Biology, University of Aveiro, 3810-193 Aveiro, Portugal

HIGHLIGHTS

- Overpotential of NiFe LDHs was 333–411 mV_{RHE}, lower than for RuO_2 (507 mV_{RHE}).
- Increase in LDH crystallinity led to an increase in OER overpotential.
- OER overpotential did not change for Ni/Fe ratio between 2:1 and 4:1.
- O_2 measurements with microelectrode revealed a non-tafelian behaviour of NiFe LDHs.

GRAPHICAL ABSTRACT

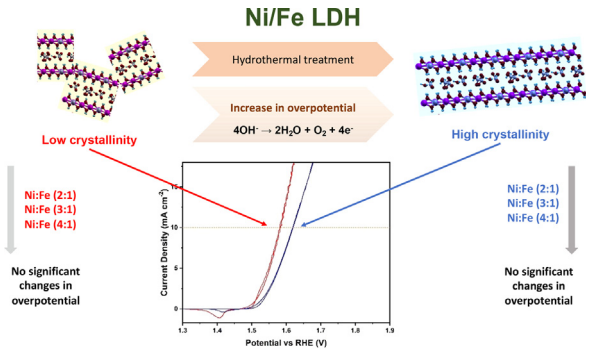

ARTICLE INFO

Article history:
Received 25 June 2021
Revised 18 October 2021
Accepted 18 October 2021
Available online 23 October 2021

Keywords:
Oxygen Evolution Reaction
Electrocatalysis
Layered Double Hydroxides
Overpotential
Crystallinity

ABSTRACT

The Oxygen Evolution Reaction (OER), half-reaction of the water-splitting process for hydrogen production, suffers from sluggish kinetics. NiFe materials appeared as interesting catalytic materials for this reaction in alkaline electrolyzers and have been studied, particularly in the form of NiFe Layered Double Hydroxides (LDH). However, the impact of the specificity of the atomic arrangement in the LDH and of its composition on the catalytic efficiency of the material are still unknown. Herein, LDH are synthesized with Ni/Fe ratios from 2 to 4 and different levels of crystallinity to assess their electrocatalytic behavior in 0.1 M KOH. Statistical analysis of the electrochemical results allows to highlight that, while no effect from the atomic ratio is observed, an increase in the crystallinity of the LDH seem detrimental to the catalytic efficiency.

1. Introduction

For hydrogen to become competitive compared to fossil fuels, cost effective and sustainable catalytic materials are needed for low-temperature water-electrolysis. The oxygen evolution reaction (OER) is the main limiting step of the overall water-splitting process, as it presents a large overpotential in comparison to the thermodynamic limit of 1.229 V *vs.* RHE. This is the main driving force for the current research on electrolyzers for the OER. Well-studied RuO_2 and IrO_2 present good efficiency, however, sustainability requires the replacement of these critical elements by materials containing Earth-abundant elements [1,2]. In the last decades, an increased interest appeared for mixed hydroxides of Ni and Fe for OER application, as described in the recent review of Gao and Yan [3]. These include layered double hydroxides, which structurally consist of positively-charged, brucite-like layers with edge-sharing $M(OH)_6$ octahedrons (M = Ni, Fe), charge-balanced by interlayer anions plus water molecules. These Ni-Fe layered double hydroxides (LDH) were reported to present low overpoten-

* Corresponding author.
E-mail address: joao.tedim@ua.pt (J. Tedim).

https://doi.org/10.1016/j.matdes.2021.110188
0264-1275/

tial and low Tafel slope for OER in alkaline media [4,5], which are very important catalytic indicators.

Although the particular platelet like structure of LDH is often mentioned as an advantage leading to a large surface area of the catalyst [6,7], it is not yet clear why this specific material is efficient towards OER and whether it is due to the elemental composition or to its particular structure. A better understanding of the OER reaction mechanisms is necessary to highlight the characteristics allowing faster kinetics in order to obtain an efficient design of this type of catalysts. The impact of several factors on the OER catalytic activity of Ni-Fe LDH has been evaluated, such as the Ni/Fe ratio of the cationic layer [8,9], the nature of the intercalated anion [10], or the effect of delamination of the LDH [6,11]. However, the wide range of experimental conditions and material analysis procedures reported, the lack of information to fully replicate the published works and, consequently, the scattering of results obtained in different works leads to difficult comparison of the published results. As a result, newcomers in the field can easily doubt on the main factor(s) behind the good efficiency claimed for these materials.

It is worth to mention that current alkaline electrolyzers industrially used are often Ni-based electrodes, at which surface the reaction takes place [2]. On these electrodes, a strong layer of hydroxides with different structures and level of hydration is formed upon cycling. Some groups studied the effect of different amounts of Fe in Ni hydroxides on the efficiency towards the OER, but without ever mentioning the name of LDH structure [12]. Others reported the interesting properties of combining Ni and Fe elements in electrodeposited [12], sputtered [12], or chemically bulk-synthesized hydroxides[1].

In the case of Ni-Fe in LDH structure, the observation we made is that the literature rarely considers and discuss the importance of both the ratio and the crystallinity of the catalyst in a single work, or at least not explicitly, which is the objective of this work.

As regards to the ratio of metallic cations, Oliver-Tolentino *et al.* reported the bulk preparation of Ni-Fe LDH of M^{II}/M^{III} ratios 1.5 and 2, obtaining better efficiency towards OER with ratio 1.5, containing more Fe, which is considered to allow the activation of Ni centers by partial-charge transfer mechanism [8]. Zhou *et al.* prepared Ni-Fe samples with different ratios, from pure Ni hydroxide to Fe oxide [9]. Of all these compositions, we consider that only the sample with M^{II}/M^{III} ratio of 2 can be considered to have a LDH structure and it is the one that presented the highest efficiency on their work. Later, Görlin *et al.* studied nanosized Ni-Fe oxyhydroxides catalysts of different metallic ratios and obtained an optimal activity towards OER for a M^{II}/M^{III} ratio of 0.8 [13]. They suggested that the good OER efficiency of the catalyst was related to the distortion of the matrix around the metallic active sites [13].

These two last works open the discussion on the role of the structure and the atomic ordering of the material. It is well known that, for any catalyst, the arrangement of the atoms and structure of the material play an important role in its electrochemical behavior. In particular, it is commonly accepted that a low degree of crystallinity can lead to high amount of defects which are considered to be good active sites [14]. Hall *et al.,* when reviewing $Ni(OH)_2$ materials [15], verified that the reasons for this increased efficiency are still uncertain, being not clear whether the electron vacancies are induced by impurities or by high level of disorder. Electrodeposited Ni-Fe hydroxides [16] and sprayed Ni-Fe oxides [17] with amorphous structures are claimed to be very good catalysts thanks to the rough surfaces, high structural disorder and improved charges transfer rate resulting from the low order range nature of the material. Regarding the Ni-Fe LDH, the crystallinity of these materials is still poorly studied. Only three papers are reported in the review of Diogini and Strasser in 2016 under this topic [18]. Trotochaud *et al.* prepared amorphous electrodeposited Ni-Fe oxyhydroxide subjected to electrochemical aging, leading to an increase of long range order perpendicular to the metal cation sheets [19]. In the electrochemical tests, they obtained no clear difference of OER efficiency with or without aging, which led them to the conclusion that the long range order had no impact on the activity of the material and that structural defects did not enhance the activity [19]. This conclusion is in line with the work of Song *et al.,* who prepared highly crystalline LDH to then exfoliate them to obtain single sheets (no stacking of the metal hydroxides sheets) [11]. Although the ordering within the 2D layer was not mentioned, they got a noticeable increase in efficiency, which was not entirely due to the increase in electrochemical surface area of the material and which may be due to a higher amount of edges giving a different electronic configuration of the active sites, similarly to defects. Later, the work of Xu et al. focused on the effect of the intercalated anion and the crystallinity of the LDH on the efficiency towards OER [20]. They used a Ni/Fe ratio of 3 and observed that the higher crystallinity led to a decrease of efficiency. Nevertheless, the smaller size of the lengthly hydrothermally treated particles also induced a higher surface area which may be the cause of the improvement. In the work of Xiong *et al.,* highly crystalline LDH were prepared and then reduced to create defects through oxygen vacancies allowing better performance [21]. Thus, based on this literature review, it is possible to wonder to which extent is the LDH ordered structure, with its characteristic platelet morphology, relevant towards OER, when compared to a disordered Ni/Fe oxyhydroxide.

To help answer this question, the present work gives insights on the importance of the ratio and crystallinity of the Ni-Fe LDH catalyst for its efficiency towards the OER. The approach followed to extract the electrochemical performance parameters can be divided into three main parts. First, the experimental setup and measurements carried out were validated using RuO_2 as benchmark. This intends to prove that the conditions in which the measurements were done are line with the literature. Second, NiFe LDHs prepared with different degrees of crystallinity and Ni/Fe ratios were characterized using a method proposed by McCrory et al [22,23]. This part aims to generate data that can be directly compared with other works performed under the same conditions, thereby reducing differences in performance resulting from the breath of experimental conditions used for the preparation of the electrodes and not of the electrocatalyst properties *per se*. Third, the data obtained, namely overpotential and Tafel slopes, were not just reported but critically analyzed: in the case of overpotential values, statistical analysis was performed in order to identify trends beyond random fluctuations, while in the case of Tafel slopes, O_2 measurements using microelectrodes were performed in order to unambiguously identify the region of O_2 evolution and evaluate whether Tafel slopes could be extracted or not. Altogether, this is an original approach and it is expected to shed light on the properties that can actually affect the electrocatalyic properties of NiFe LDH family towards OER, with implications on the design of electrolyzers at industrial level.

Herein, Ni-Fe LDH intercalated with carbonates were synthesized with different degrees of crystallinity through a simple hydrothermal method, for different Ni/Fe ratios. The carbonate intercalated hydroxide was chosen as it is the most stable form of Ni-Fe LDH and, hence, would present less degradation by anion-exchange in electrolytes containing potential impurities, making it an "application-friendly" catalyst. Their efficiency as catalysts for the OER was evaluated and compared with standard RuO_2 as a benchmark. The Tafel slopes and overpotentials were correlated with the structural features of the synthesized nanostructured Ni-Fe. Finally, the difficulty in comparing the electrochemical results with published data is discussed.

2. Experimental section

2.1. Synthesis

Ni-Fe/CO_3 LDH were synthesized using co-precipitation method in aqueous solution to obtain materials with a Ni/Fe ratio of 2, 3 and 4 [8,24]. The LDH were prepared by dropwise addition of an aqueous solution (25 mL; pH = 12.5) of NaOH (1.17 M) and Na_2CO_3 (0.34 M) to an aqueous solution (25 mL) of nitrate metallic salts (0.5 M), under vigorous stirring at room temperature. The metallic salt solution was prepared with the desired Ni/Fe ratio. After complete addition, the resulting brownish slurry was stirred for two hours (final pH = 9). Half of the slurry volume is kept aside and called Ni/Fe*x*-AsPrep (*x* = Ni/Fe ratio). The rest of the slurry was thermally treated in an autoclave at 120 °C for 24 h and named Ni/Fe*x*-HT. All six samples were rinsed with DI water and centrifuged 3 times to eliminate any salt residues.

2.2. Materials characterization

The LDH slurries were dried overnight in oven at 80 °C and ground to a fine powder. The powder X-Ray diffraction was recorded using a PANalytical Xpert Pro instrument with Cu K_α radiation (λ = 1.5418 Å) and graphite monochromator. Phase analysis was performed using the PDF-4 + 2019 database from the International Center for Diffraction Data. The profile matching of the obtained pattern was performed with the FullProf software, using a cell of space group R-3 m (166).

The morphology of the materials was observed by Scanning Electron Microscopy with a Hitachi S-4100 system using an electron beam energy of 25 keV. The sampling was made by drop-casting a suspension of the LDH powder on a Si wafer. LDH samples were also analyzed by HR-TEM, using a transmission electron microscope energy-filtered TEM EF 200 kV, JEOL brand, model 2200FS, high-resolution electron gun Schottky emission (SE), omega type energy filter column spectrometry with electron energy loss EELS.

The particles sizes and Zeta potentials were measured with a Malvern ZetaSizer Nano ZS apparatus and LDH dispersions prepared from dried powders and sonicated at least 5 min in water to ensure good particles dispersion.

Attenuated total reflectance infrared spectra of dry LDH powders were collected with a Bruker Optics tensor 27 Fourier Transform-IR spectrometer, equipped with a Golden Gate ATR accessory plate. The spectra were collected at room temperature in ambient air, and 128 scans were averaged for each sample.

Atomic Absorption Spectroscopy was performed on the samples dissolved in HCl (37 %) using an Avanta apparatus from GBC Scientific equipment with an air-acetylene flame to measure the amount of Fe (Lamp: 248.3 nm at 6 mA, with slit of 0.2 nm) and Ni (Lamp: 232.0 nm at 5 mA, with slit of 0.2 nm).

2.2.1. Electrochemical characterization

2.2.1.1. Preparation of modified electrodes. A glassy carbon rotating disk electrode (GC RDE) with 3 mm diameter was used as supporting electrode after being polished successively with SiC papers (P2500 and P4000) and suspensions of alumina powder (1 μm and 0.3 μm particle size), rinsed and sonicated 2 min in DI water after each polishing and dried in air. Aqueous suspensions of catalysts (0.5 mg mL^{-1}) were prepared from the LDH powder and sonicated 30 min. The glassy carbon RDE were modified by drop-casting the suspension (11 μL) and let dry 30 min in air, giving a final catalyst loading of 28 μg cm^{-2}. The RDE was then covered with a thin film of ion conductive polymer by drop-casting a Nafion solution (11 μL of 5 wt% Nafion® perfluorinated resin solution from Sigma-Aldrich diluted 100 times in ethanol) and let to dry 5 min at room temperature to avoid the detachment of the catalyst. The electrode was then installed as prepared in the electrochemical cell. A powder of ruthenium (IV) oxide (Alfa Aesar), deposited with the same procedure on the electrode, was used as a benchmarked electrocatalyst to evaluate the performance of the synthesized Ni-Fe LDH.

2.2.1.2. Electrochemical setup. The electrochemical experiments were performed using an Autolab PGSTAT 302 N potentiostat with the GPES software. The measurements were carried out at room temperature, inside a Faraday cage, in a cell with three-electrode configuration, with the GC RDE as working electrode, a saturated calomel electrode (SCE) as reference and a Pt wire as counter electrode. The testing electrolyte was 0.1 M KOH electrolyte. Before each experiment oxygen was bubbled in the cell for at least 20 min and the RDE rotated at 1600 rpm driven by an Autolab rotator and motor controller. The electrochemical characterization followed McCrory *et al.* [22,23]. A conditioning stage was performed consisting of 20 cyclic voltammetry sweeps in the 0–0.8 V *vs.* SCE potential range at a scan rate of 10 mV s^{-1}. This step allowed the stabilization of the catalyst and Nafion layers, verified by at least 5 identical last scans. Then, three cycles were measured at 5 mV s^{-1} between 0 and 0.8 V *vs.* SCE to extract the figures of merit: overpotential and Tafel slope. The stability of the modified electrode was tested by chrono-potentiometry for 2 h at 10 mA cm^{-2}. All polarization potentials reported are relative to the reversible hydrogen electrode (RHE) and current densities per geometric area (0.196 cm^2). The small catalyst loading and the fact of being impregnated in Nafion, prevented the use of XRD or XPS to verify compositional and structural changes after the experiments, as discussed in other works [25].

2.2.1.3. Statistical analysis. Electrochemical data (overpotential values; n = 5 per each material) was submitted to statistical analysis. Data normality and homoscedasticity were previously tested using Shapiro-Wilk and the Spearman tests ($p < 0.05$), respectively. A two-way analysis of variance was then used to compare the statistical OER differences among synthetized materials, considering the factors "treatment type" and "Ni/Fe ratio", followed by the Tukey's multiple comparison test, whenever significant differences were observed ($p < 0.05$). The statistical analysis was performed with the software Prism version 8.

3. Results

Ni-Fe/CO_3 LDH were synthesized by co-precipitation with a Ni/Fe ratio of 2, 3 and 4. Part of the powders were further subjected to a hydrothermal treatment (HT). As such, six samples were produced, three resulting directly from the synthesis, and named Ni/FeX-AsPrep, and three coming from the HT and named Ni/FeX-HT (where X = Ni/Fe ratio)

3.1. Material characterization

The aspect of the prepared materials is observed by scanning electron microscope (SEM) (Fig. 1). The as-prepared samples present aggregates of poorly defined shapes, while the heat-treated samples display individual platelets with approximate hexagonal shape, as reported for several LDH-type materials [26–28]. More particularly, the sample Ni/Fe4-HT has the aspect of a desert rose, probably due to the higher content of Ni, as this morphology is characteristic of some $Ni(OH)_2$ materials [15].

The average particle size (Z-Ave) of the studied LDH dispersed in deionized water, which is presented in Table 1, varied between

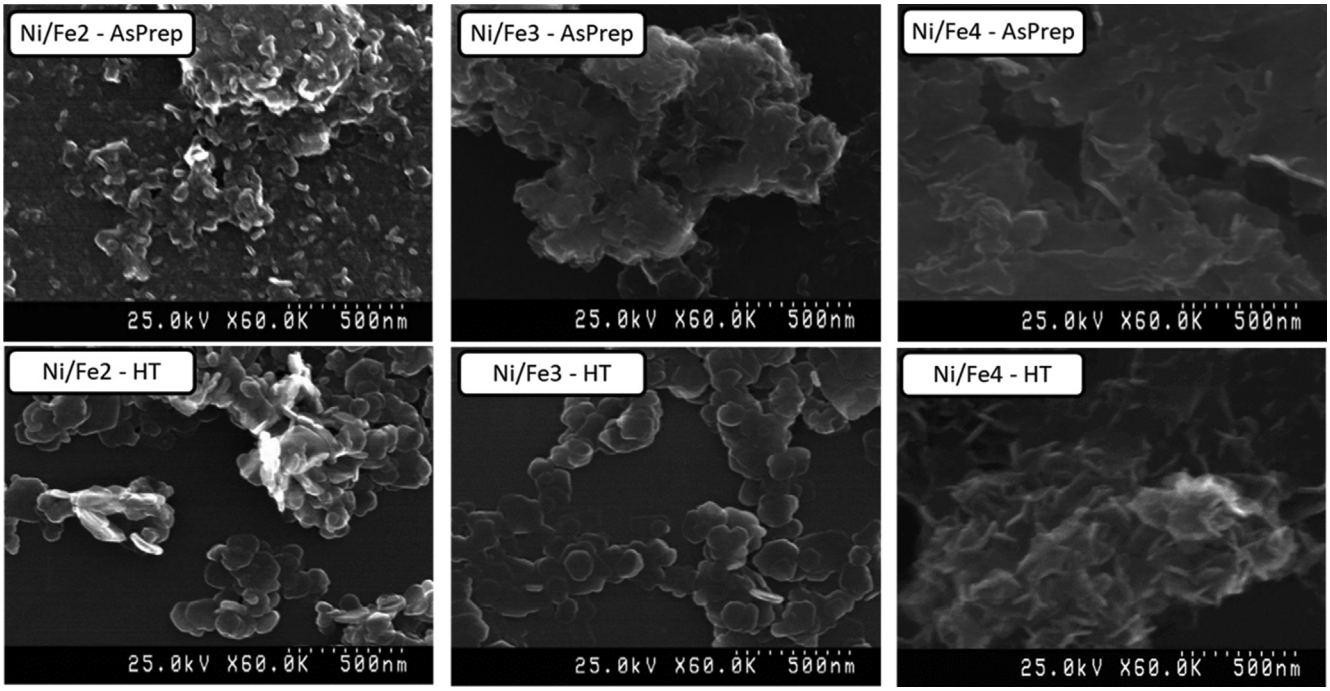

Fig. 1. SEM study of the morphology of the LDH particles of Ni/Fe ratios of 2, 3 or 4 and as-prepared or with hydrothermal treatment (24 h at 120 °C).

Table 1
Dynamic Light Scattering (Z-Average values) and zeta-potential measurements on the dispersions of the LDH of Ni/Fe ratios of 2, 3 or 4 and as-prepared or with hydrothermal treatment (24 h at 120 °C).

Sample	Z-Ave		ZP	
	d.nm	Std. dev.	mV	Std. dev.
Ni/Fe2-AsPrep	490	41	+45	3
Ni/Fe2-HT	242	5	+40	1
Ni/Fe3-AsPrep	758	42	+43	2
Ni/Fe3-HT	432	16	+51	1
Ni/Fe4-AsPrep	527	107	+40	4
Ni/Fe4-HT	568	126	+41	1

242 nm and 758 nm. These values should be considered more as an order of magnitude than as the exact particle sizes, because the particles have platelet-like shape and not the spherical form required by the dynamic light scattering theory [29]. Moreover, the measured entities seem to have been mainly aggregates composed of smaller particles, appearing on SEM images with widths between 50 nm and 250 nm. Table 1 also presents the zeta potential (ZP) of the particles. The values ranged between + 40 and + 50 mV, allowing for the stabilization of a dilute suspension of particles in deionized water due to electrostatic repulsions (concentration < 0.1 mg mL^{-1}), which is important for preparing well dispersed suspensions of LDH for the electrochemical measurements.

The attenuated total reflectance infrared (ATR-FTIR) measurements (Fig. 2) confirm the presence of CO_3^{2-} in the LDH samples, with a strong absorption band at 1350 cm^{-1}. The large band around 3500 cm^{-1} corresponds to O-H stretching and the one at 1630 cm^{-1} to the H-O-H deformation, showing qualitatively the hydration of the LDH samples. Bands under 1000 cm^{-1} correspond to bonds between oxygen and metallic atoms forming the hydroxide layers [30].

The results of the chemical analysis of the dissolved materials through atomic absorption spectroscopy (AAS) are displayed in Table 2. The molar ratios of the synthesized materials correspond

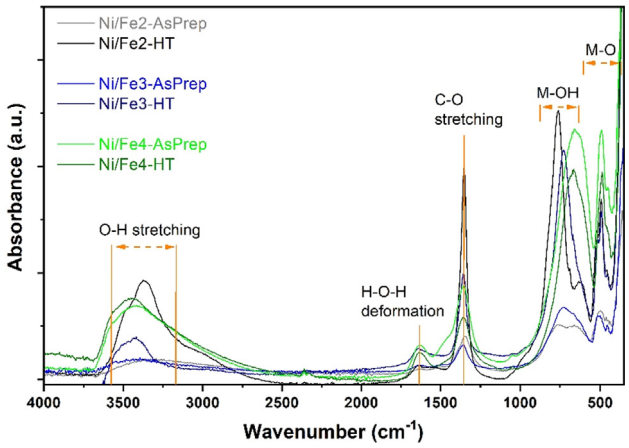

Fig. 2. FTIR measurement of the six synthesized samples with highlights of the main bands observed in LDH structures.

Table 2
Chemical composition: Determination of Fe and Ni weight content of each sample by AAS and calculated molar ratio.

Sample	wt% of Fe	wt% of Ni	Molar Ni/Fe ratio
Ni/Fe2-AsPrep	15.4	30.9	1.9
Ni/Fe2-HT	14.3	38.6	2.6
Ni/Fe3-AsPrep	11.0	34.4	3.0
Ni/Fe3-HT	11.4	33.7	2.8
Ni/Fe4-AsPrep	8.5	36.6	4.1
Ni/Fe4-HT	8.6	36.0	4.0

to the expected ones, except for the sample Ni/Fe2-HT. The solution of Ni/Fe2-HT contained some undissolved particles remaining, corresponding to an oxide phase, which was hence not analyzed with the rest of the solution, leading to a lower amount of Fe measured than for Ni/Fe2-AsPrep. This observation proves that the LDH

phase obtained in the case of the Ni/Fe2-HT has a higher Ni/Fe ratio than expected.

Fig. 3**a** displays the X-ray diffraction patterns for the three compositions investigated in this work, both as-prepared and after hydrothermal treatment. The pattern is matched with the peaks corresponding to the rhombohedral structure of Iron-Nickel Carbonate Hydroxide Hydrate of formula $Ni_6Fe_2(OH)_{16}(CO_3)\cdot 4H_2O$ (computed pattern JCPDS 01–082–8040). The peaks (003), (006) and (009) are characteristic of the layered structure of the 3R LDH polytype, from which can be extracted the basal spacing of 7.7 ± 0.15 Å, typical of a carbonate-intercalated LDH [28]. The sample Ni/Fe2-HT has a pattern with more defined peaks in the region 2θ = 35° to 60°. This region corresponds to the reflections of the interlayer, which let us suppose that the molecules forming the interlayer are more ordered in this sample.

For each sample, the average crystallite size in the *a* direction is estimated by the Scherrer equation using the full width at high maximum of the (110) peak, determined by fitting together (110) and (113), often overlapped. The obtained crystallite sizes are ranging between 8 and 33 nm (Fig. 3b). It is worth to note that these values are a low-end estimate of the actual crystallite sizes, as the broadening of the diffraction peak can be due to local imperfections in the lattice such as strain and chemical heterogeneities. As expected, the crystallite size increased after hydrothermal treatment, for all the Ni-Fe LDH compositions considered in this work. Moreover, bigger crystallite sizes were obtained for samples with lower Ni/Fe ratio, which suggest a link between the amount of M^{III} cations in the structure and the propensity of the hydroxide layers to stack more regularly. In the case of well-defined hexagonal platelets for Ni/Fe2-HT and Ni/Fe3-HT visible on SEM pictures, the actual crystal sizes correspond to the width of the platelets, which is ranging between 80 and 120 nm, meaning 3 to 15 times the estimated crystallite sizes. Hence, the values estimated through the Scherrer equation are not to be considered as the actual size of the LDH crystal but as a parameter to assess the quality of the long-range order of the structure.

To explore further the crystallinity of the samples, the profile matching of the diffraction patterns was performed using the FullProf software using a R–3 m symmetry to extract the cell parameters. Both parameters *a* and *c* were found to increase with the Ni/Fe ratio (Fig. 3c). This is consistent with the size of the cations, as the bivalent nickel is 0.08 Å bigger than the trivalent iron, according to the Shannon tables [31]. The *c* parameter increases with the Ni/Fe ratio, which is also consistent with the fact that the layers are less positively charged and hence, the attraction between layer and interlayer is smaller, leading to a less "compact" stacking.

The XRD pattern of the sample Ni/Fe2-HT presents additional peaks which do not correspond to the Ni-Fe carbonate hydroxide structure (Fig. 3a). Such pattern has also been observed in other works synthesizing Ni-Fe LDH by hydrothermal technique [24,32] and were assigned to the spinel structure of the $NiFe_2O_4$ phase (JCPDS: 00–054-0964). The hydrothermal treatment in autoclave, carried out with the aim to enhance the growth of the LDH particles, promoted the segregation of an iron-rich phase. A similar work, where the material is thermally treated under lower conditions of temperature (50 °C) and pressure does not present the $NiFe_2O_4$ phase [8], which shows that this segregation is due to the higher temperature applied to the sample. It is worth of men-

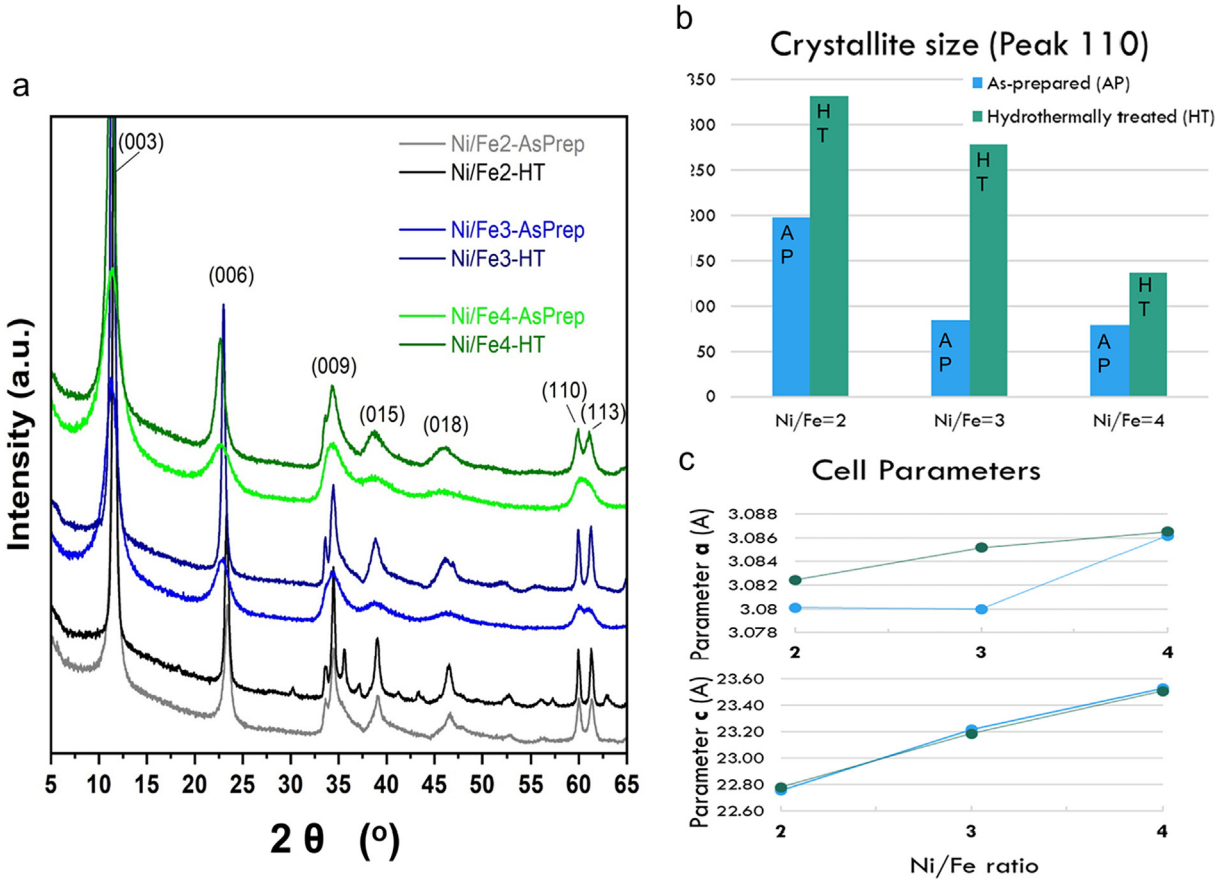

Fig. 3. a) Powder XRD patterns of the prepared samples. b) Crystallite size in *a* direction [peak (110); units: Å]. b) Cell parameters (*a* and *c*) extracted from the XRD results (units: Å).

tion that the spinel structure is consistent with the presence of insoluble particles found when dissolving the Ni/Fe2-HT sample for AAS measurements was attempted (cf. Table 2).

Transmission electron microscopy (TEM) was used to more clearly identify some features evidenced in SEM and XRD analyses. TEM images depicted in Fig. 4 reveal that the obtained Ni-Fe LDHs present a plate-like morphology, with some hexagonal shapes being identified, especially for samples subjected to hydrothermal treatment (Ni/Fe2-HT, Ni/Fe3-HT, Ni/Fe4-HT). Moreover, particle size of individual particles increases after hydrothermal treatment.

The sample Ni/Fe2-HT, which revealed a secondary phase by XRD (recall Fig. 3), actually presents a few particles which have different shape and density (highlighted with an orange circle in Fig. 4). This could be associated with the $NiFe_2O_4$ formed after hydrothermal treatment. However, it must be mentioned that due to the overlapping of these particles with LDH particles, diffraction analysis could not be performed to unambiguously identify this secondary phase.

3.2. Electrochemical characterization

Cyclic voltammograms (CV) obtained for the neat glassy carbon electrode, the RuO_2 benchmark and the LDH samples are displayed in Fig. 5 after ohmic drop correction of the data. The glassy carbon substrate presents no current in the studied potential range. The electrochemical procedure was first validated by experiments using commercial RuO_2 powder as a benchmark. Working electrodes were prepared following the procedure reported by Jung *et al.* with commercial RuO_2 [22], with a catalyst loading of 800 μg cm^{-2}. We obtained a similar Tafel slope (67 mV dec^{-1}) and an overpotential of 290 ± 11 mV, lower than the reference value (the overpotential at 10 mA cm^{-2} was 380 ± 20 mV and the Tafel slope was 65 mV dec^{-1}) [22]. Following these tests, the LDH loading was reduced to 28 μg cm^{-2} in order to obtain a stable film, not possible with the 800 μg cm^{-2} loading.

The CVs of the different prepared electrodes (Fig. 5) exhibit an increasing catalytic current for potentials more positive than 1.5 V *vs.* RHE, corresponding to the onset of the OER. In comparison, the electrode prepared with RuO_2 showed a catalytic current lower than the LDH samples, leading to an overpotential of 500 mV at 10 mA cm^{-2}. The curves of the LDH are very similar to one another, however, the current slope corresponding to the OER was higher for AsPrep samples, leading to lower overpotentials at 10 mA cm^{-2} compared to the hydrothermally treated samples. In the case of LDH with a Ni/Fe ratio of 4, an additional wave appeared at 1.49 V (Ni/Fe4–AsPrep) and 1.52 V (Ni/Fe4-HT), which was attributed to the Ni^{II}/Ni^{III} oxidation [8]. In samples with lower Ni/Fe ratio, this feature is less visible due to the lower Ni content and to its overlapping with the OER peak. Confirming the change of the Ni state at this potential, a change of color from light to dark brown was detected, more perceptible in the materials with higher Ni. In the reverse scan, the Ni^{III}/Ni^{II} reduction peak appeared in each Ni/Fe LDH sample, from 1.43 V to 1.40 V, in the order Ni/Fe2-HT > Ni/Fe2-AsPrep > Ni/Fe3-HT > Ni/Fe3-AsPrep > Ni/Fe4-HT > Ni/Fe4–AsPrep. This order may illustrate the availability of Ni atom in each LDH for changing its oxidation state upon polarization.

In the E *vs.* log(i) plots of the cyclic voltammetry data obtained for each of our samples (Fig. 6**a**), different regions are visible. The main linear region appears at low currents (0.01 to 1 mA cm^{-2})

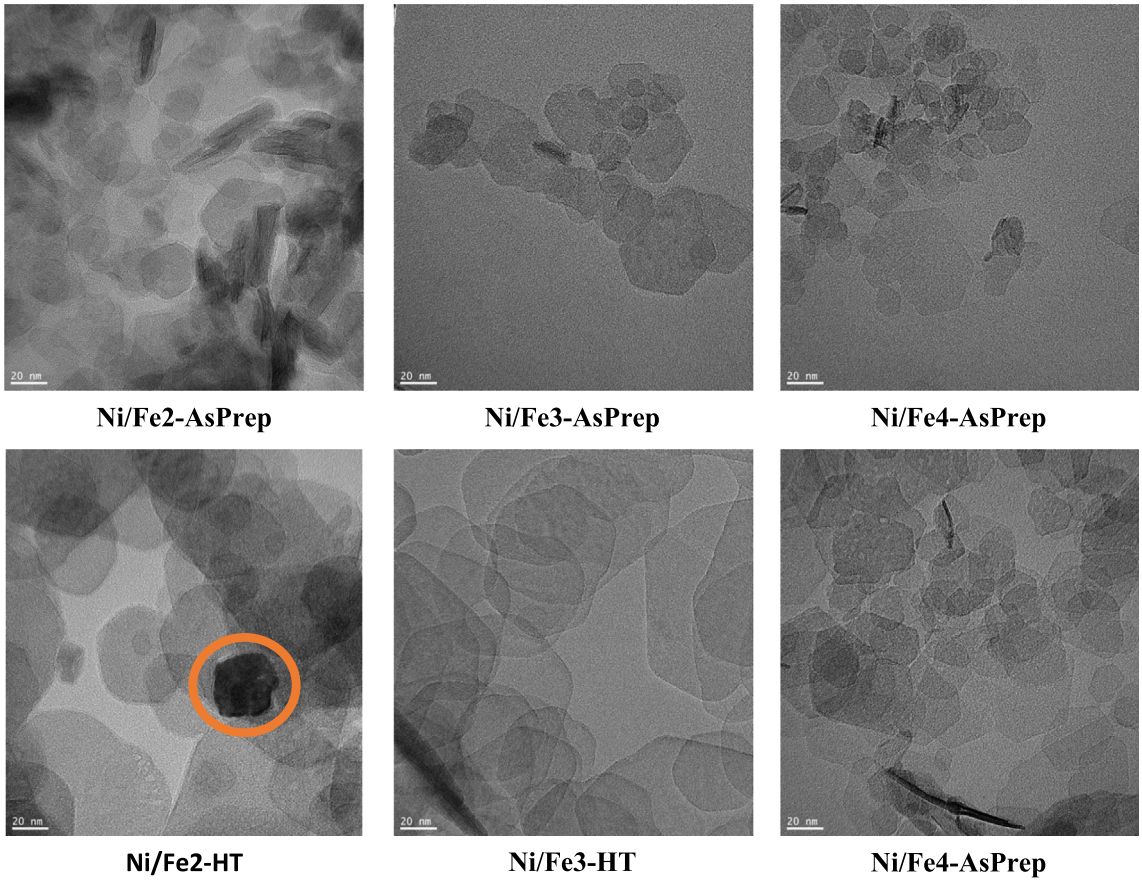

Fig. 4. TEM Images of Ni-Fe LDHs. Orange circle in the TEM image of Ni/Fe2-HT highlights particles with different shape and density, that can be associated with secondary phase detected by XRD.

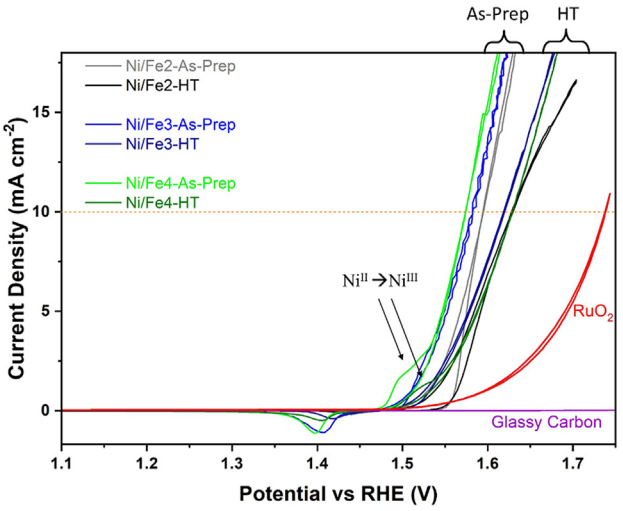

Fig. 5. Cyclic voltammetry measurements of the glassy carbon substrate, the RuO_2 reference and LDH particles of Ni/Fe ratios of 2, 3 or 4 and as-prepared or with hydrothermal treatment (24 h at 120 °C).

and is identified with red lines in the graph. It is attributed to the oxidation of Ni^{II} to Ni^{III}, with a low Tafel slope, between 20 and 30 mV dec^{-1}, highlighting the fast reaction kinetics. To confirm that OER was taking place at higher potentials, the voltammograms were repeated with an O_2 micro-sensor close to the electrode surface for detecting the potential at which O_2 was formed. For these experiments the glassy carbon electrode did not rotate and was facing up. The micro-sensor was a 10 μm platinum disk polarized at a potential were O_2 is reduced with limiting control (in this experiment −0.8 to −1 V *vs* SCE). The idea is that the current measured by the microelectrode will be constant and proportional to the concentration of dissolved O_2 in the bulk solution but should immediately increase as soon as O_2 starts to be generated in the glassy carbon electrode with catalyst. The result is presented in Fig. 6 b) and shows the superposition of the current measured in the GC electrode with LDH catalyst and the current measured by the O_2 sensing microelectrode. The × axis depicts the potential at the GC. The O_2 reduction current measured at the microelectrode is negligible until the GC potential reaches 0.5 V *vs* SCE. Then, for more positive potentials, the current increases rapidly until the saturation of the measuring device (1 nA) is reached. This experiment was performed with all LDH samples and confirmed that O_2 was produced at potentials higher than the linear region of the Tafel plot. In these plots, the region corresponding to the OER does not present a Tafelian behavior, making difficult its determination with confidence. This supports the suggestion of McCrory *et al.* about the possible change of reaction mechanisms with change of potential [23]. Based on these findings it was decided to not use in this work the Tafel slope as a figure of merit to assess the efficiency of the catalyst.

Fig. 6

The overpotential values measured on the ohmic drop-corrected plots at 10 mA cm^{-2} are reported in Fig. 7**a**. Each electrode was also submitted to a stability test to observe the evolution of the overpotential while applying a current of 10 mA cm^{-2} for two hours (Fig. 7b). No important degradation of the electrodes has been observed as the increase of the overpotential was kept under 50 mV for all electrodes. The mean overpotentials varied between 330 mV and 410 mV. These values are higher than the reported for the best materials [4,20,21], but it is important to note that in this study a low catalyst loading was used and no conductive carbon material was added to the ink. Furthermore, the aim of this paper is to compare samples in the same conditions, as the comparison with materials from other publications using the overpotential is not accurate, owing to the number of experimental parameters that can influence the results. Qualitatively, two main findings can be highlighted: (i) the overpotential decreased in the AsPrep samples with increasing Ni/Fe ratio and (ii) the overpotential of the Ni/FeX–HT samples was larger for any of three Ni/Fe ratios surveyed, which seems to indicate that the higher crystallinity due to the hydrothermal treatment leads to lower efficiency.

Fig. 7

The observations performed in the previous paragraph are based on the comparison of the mean values of the figure of merit chosen to describe the efficiency of the electrocatalysts (cf. Fig. 7a). An analysis of variance (ANOVA) of the results of the overpotential

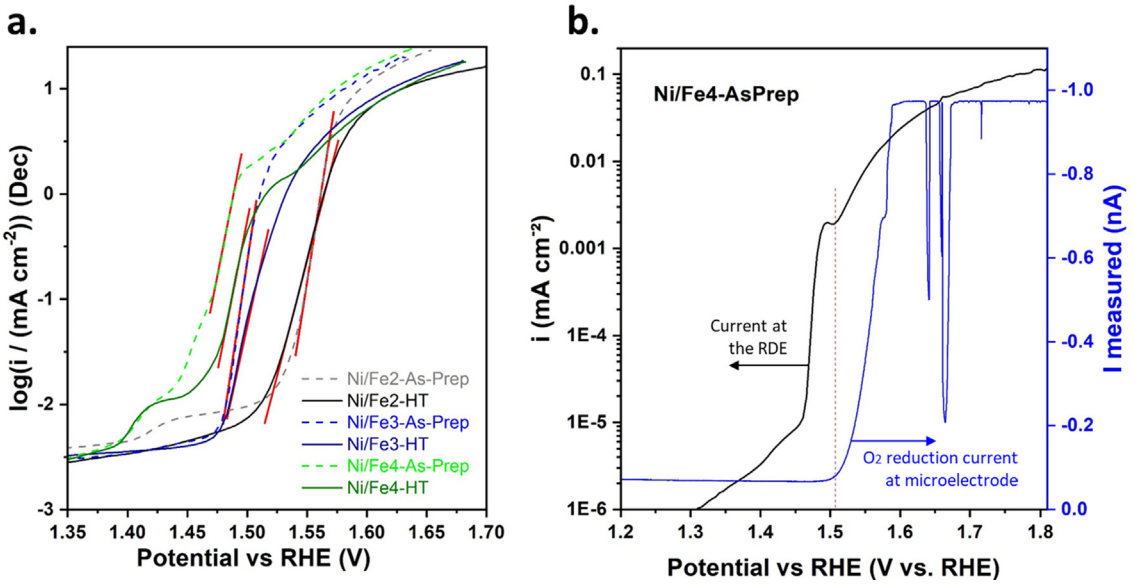

Fig. 6. a) Tafel plot of the LDH samples with different ratio and hydrothermal treatment. The linear part highlighted in orange correspond to the oxidation of Ni^{II} to Ni^{III}. b) Identification of the region were O_2 is formed (OER) in sample Ni/Fe4-AsPrep with the help of an O_2 microsensor.

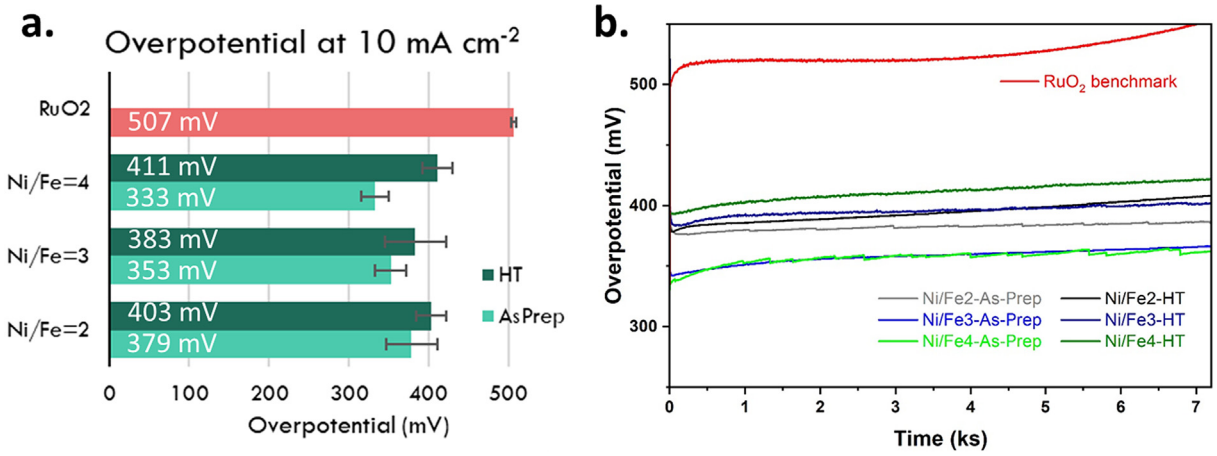

Fig. 7. a) Average overpotential extracted from CV curves. b) Chronopotentiometric tests of the electrodes at a current of 10 mA cm^{-2}.

was performed using the 2-way ANOVA test to evaluate the effect of the hydrothermal treatment and of the Ni/Fe ratio. To the best of our knowledge, no study on NiFe LDH for OER catalysis takes into consideration the importance of samples replication and the data variability. In the present study, five replicates of electrode for each LDH were tested, from which we extract the overpotential value. The assumptions of data normality and homoscedasticity were successfully verified through Shapiro-Wilk and Spearman's test, respectively, before performing the 2-way ANOVA tests. The ANOVA statistical analysis highlighted the effective impact on the thermal treatment on the catalyst efficiency: a hydrothermally treated LDH sample is more crystalline and present a significantly higher overpotential than its non-treated counterpart ($F_{(1,24)}$ = 22.48, p < 0.0001), while the Ni/Fe ratio caused no statistically relevant differences in measured OER values ($F_{(2,24)}$ = 2.29, p = 0.1225) (pls. cf. Table S1).

The Tukey's multiple comparison test showed that there is difference in the overpotential values measured between samples of Ni/Fe4 LDH AsPrep *vs.* HT (pls. cf. Table S1). No significant overpotential differences were found in the comparison AsPrep *vs.* HT for the other two ratios, neither between samples with similar hydrothermal treatment and different ratios (pls. cf. Table S1).

This study raises awareness about results reported in the literature taking conclusion on the impact of metal ratios or crystallinity of the sample without mentioning repeatability of the electrochemical measurements. The preparation of the working electrode can have as much impact as the difference of Ni/Fe ratio in the ranges studied in this work.

4. Discussion

Firstly, the electrochemical characterization presented in section 3 highlights that the layered double hydroxides prepared in this work present a lower overpotential than the RuO_2 reference material, justifying once again the efforts in better understanding and developing NiFe electrocatalyst LDHs.

Then, when comparing samples within AsPrep or HT group separately, we observe that the increase of Ni/Fe ratio implies an increase in the cell parameters *a* and *c* linked with a decrease of the positive charge of the LDH layer due to less divalent Fe atoms. Many references [8,9,13], report a better efficiency for lower Ni/Fe ratios (1.5, 2 and 0.8 respectively), as if a higher concentration of Ni would be unfavorable for the catalyst efficiency. However, from the results of this study, the changes in composition and structure do not introduce significant electrocatalytic differences.

On the other hand, the statistical analysis of the electrochemical data shows that using a more crystalline material on the electrode results in a lower electrocatalytic performance. In our work, it was seen for NiFe4-AsPrep *vs.* NiFe4-HT but less clearly for lower Ni/Fe ratios. These results are consistent with a work reported by Xu *et al.* in 2015, which shows, through the comparison of overpotentials, that a LDH material with a Ni/Fe ratio of 3 presents lower efficiency when it is hydrothermally treated, mentioning that lower crystallinity provides less confined active sites [20]. However, the discussion does not make the distinction between the atoms ordering and the size of the LDH particles inducing a higher surface area, which could be the cause for the improvement. Another work, from Gao *et al.* also concludes that the amorphous nature of the material makes it more flexible and hence more stable over time to electrochemical processes in comparison to crystalline materials [16], although their material is preconditioned for a long time to achieve the higher catalytic efficiency, which eventually may lead to a rearrangement of the material in more stable phases. The interest of defects for electrocatalysis is also discussed in the work of Trotochaud *et al.,* in 2014, which mentions that the increase of efficiency of a β-$(NiOH)_2$ is due to the inclusion of Fe impurities, and not to the more ordered structure than in the α-$(NiOH)_2$ [19]. They conclude that the long-range order in the material seems unimportant. Görlin *et al.* discussed this point in a work on nanosized Ni-Fe oxyhydroxides catalysts of different metallic ratios and highlighted that the higher OER efficiency of the catalyst is related to the distortion of matrix around the metallic active sites [13]. Hence, from the results obtained and what is seen in the literature, it seems that more disordered material is more efficient, in terms of overpotential.

Mostly, the present study reinforces that the importance of the LDH phase in the NiFe mixed hydroxide lies in the fact that this structure allows a "*meta*-stable" phase of the hydroxide, preventing phase segregation, but the long-range order or the platelet-like morphology does not seem necessary and would even be detrimental for the electrochemical efficiency of the material. In parallel, the effect of the metallic cation ratio is not clear. More fundamental studies would help determine if the discussion of the influence of the Ni/Fe ratio is overrated as a single factor or if it is a combination of the presence of Fe with a distorted β-$Ni_2(OH)$ structure that can be the right direction for the development of better NiFe-based electrocatalysts.

From an application-based point of view, the statement that the hydrothermal treatment is detrimental for the catalytic efficiency is interesting as it allows to remove a time and energy-intensive step from the catalyst production process.

On a more general note, there are several recent works in the literature reporting promising eletrocatalysts for different reactions [33–35]. The strategy followed in this work could be extended in a general way to the design of similar materials.

5. Conclusions

This work exposes views on the currently highly studied NiFe layered double hydroxides for efficient catalysis of the OER. Both the Ni/Fe ratio and the crystallinity of the synthesized material are investigated to highlight their influence on the electrocatalytic activity of the Ni/Fe LDH. No evidence was found for any impact of the Ni/Fe ratio in the efficiency of the OER but the hydrothermal treatment performed to obtain a higher crystallinity of the catalysts leads to a decrease of their efficiency. In conclusion, this work renders insights on the structure and Ni/Fe ratio, which are relevant for the design of NiFe LDHs. Future works will involve the use of other catalyst supports to increase the loading of catalyst and test the material closer to the application conditions, namely using larger current densities.

Data availability

The raw/processed data required to reproduce these findings cannot be shared at this time as the data also forms part of an ongoing study.

Declaration of Competing Interest

The authors declare that they have no known competing financial interests or personal relationships that could have appeared to influence the work reported in this paper.

Acknowledgments

Thanks are due to FCT/MCTES for the financial support to CICECO-Aveiro Institute of Materials (UIDB/50011/2020; UIDP/50011/2020) and CESAM (UIDP/50017/2020 + UID B/50017/2020), through national funds. We thank also the European Commission funding the project NANOBARRIER (Reference N°280759) through the programme FP7-NMP. This study was also carried out in the framework of the NANOGREEN R&D project (CIRCNA/BRB/0291/2019) funded by national funds (OE), through FCT. Roberto Martins and Alexandre Bastos funded by national funds (OE), through FCT – Fundação para a Ciência e a Tecnologia, I.P., in the scope of the framework contract foreseen in the numbers 4, 5 and 6 of the article 23, of the Decree-Law 57/2016, of August 29, changed by Law 57/2017, of July 19 (CEECIND/01329/2017), and in frame of SMARTAQUA project, which is funded by the Foundation for Science and Technology in Portugal (FCT), the Research Council of Norway (RCN), Malta Council for Science and Technology (MCST), and co-funded by European Union's Horizon 2020 research and innovation program under the framework of ERA-NET Cofund MarTERA (Maritime and Marine Technologies for a new Era).

Appendix A. Supplementary material

Supplementary data to this article can be found online at https://doi.org/10.1016/j.matdes.2021.110188.

References

[1] J. Luo, J.-H. Im, M.T. Mayer, M. Schreier, M.K. Nazeeruddin, N.-G. Park, S.D. Tilley, H.J. Fan, M. Grätzel, Water photolysis at 12.3% efficiency via perovskite photovoltaics and Earth-abundant catalysts, Science 345 345 (6204) (2014) 1593–1596, https://doi.org/10.1126/science:1258307.
[2] F.M. Sapountzi, J.M. Gracia, C.J. Weststrate, H.O.A. Fredriksson, J.W. Niemantsverdriet, Electrocatalysts for the generation of hydrogen, oxygen and synthesis gas, Prog. Energy Combust. Sci. 58 (2017) 1–35, https://doi.org/10.1016/j.pecs.2016.09.001.
[3] R. Gao, D. Yan, Recent Development of Ni/Fe-Based Micro/Nanostructures toward Photo/Electrochemical Water Oxidation, Adv. Eng. Mater. 10 (2020) 1900954 (1 of 19), Doi: 10.1002/aenm.201900954
[4] M. Gong, Y. Li, H. Wang, Y. Liang, J.Z. Wu, J. Zhou, J. Wang, T. Regier, F. Wei, H. Dai, An Advanced Ni–Fe Layered Double Hydroxide Electrocatalyst for Water Oxidation, J. Am. Chem. Soc. 135 (23) (2013) 8452–8455, https://doi.org/10.1021/ja4027715.
[5] X. Long, J. Li, S. Xiao, K. Yan, Z. Wang, H. Chen, S. Yang, A Strongly Coupled Graphene and FeNi Double Hydroxide Hybrid as an Excellent Electrocatalyst for the Oxygen Evolution Reaction, Angew. Chemie Int. Ed. 53 (29) (2014) 7584–7588, https://doi.org/10.1002/anie.201402822.
[6] K. Yan, T. Lafleur, J. Chai, C. Jarvis, Facile synthesis of thin NiFe-layered double hydroxides nanosheets efficient for oxygen evolution, Electrochem. commun. 62 (2016) 24–28, https://doi.org/10.1016/j.elecom.2015.11.004.
[7] Y. Wang, D. Yan, S. El Hankari, Y. Zou, S. Wang, Recent Progress on Layered Double Hydroxides and Their Derivatives for Electrocatalytic Water Splitting, Adv. Sci. 5 (8) (2018) 1800064, https://doi.org/10.1002/advs.v5.810.1002/advs.201800064.
[8] M.A. Oliver-Tolentino, J. Vázquez-Samperio, A. Manzo-Robledo, R.d.G. González-Huerta, J.L. Flores-Moreno, D. Ramírez-Rosales, A. Guzmán-Vargas, An Approach to Understanding the Electrocatalytic Activity Enhancement by Superexchange Interaction toward OER in Alkaline Media of Ni–Fe LDH, J. Phys. Chem. C 118 (39) (2014) 22432–22438, https://doi.org/10.1021/jp506946b.
[9] L.-J. Zhou, X. Huang, H. Chen, P. Jin, G.-D. Li, X. Zou, A high surface area flower-like Ni–Fe layered double hydroxide for electrocatalytic water oxidation reaction, Dalt. Trans. 44 (25) (2015) 11592–11600, https://doi.org/10.1039/C5DT01474C.
[10] B.M. Hunter, W. Hieringer, J.R. Winkler, H.B. Gray, A.M. Müller, Effect of interlayer anions on [NiFe]-LDH nanosheet water oxidation activity, Energy Environ. Sci. 9 (5) (2016) 1734–1743, https://doi.org/10.1039/C6EE00377J.
[11] F. Song, X. Hu, Exfoliation of layered double hydroxides for enhanced oxygen evolution catalysis, Nat. Commun. 5 (2014) 1–9, https://doi.org/10.1038/ncomms5477.
[12] D. Friebel, M.W. Louie, M. Bajdich, K.E. Sanwald, Y. Cai, A.M. Wise, M.-J. Cheng, D. Sokaras, T.-C. Weng, R. Alonso-Mori, R.C. Davis, J.R. Bargar, J.K. Nørskov, A. Nilsson, A.T. Bell, Identification of Highly Active Fe Sites in (Ni, Fe)OOH for Electrocatalytic Water Splitting, J. Am. Chem. Soc. 137 (3) (2015) 1305–1313, https://doi.org/10.1021/ja511559d.
[13] M. Görlin, P. Chernev, J. Ferreira de Araújo, T. Reier, S. Dresp, B. Paul, R. Krähnert, H. Dau, P. Strasser, Oxygen Evolution Reaction Dynamics, Faradaic Charge Efficiency, and the Active Metal Redox States of Ni–Fe Oxide Water Splitting Electrocatalysts, J. Am. Chem. Soc. 138 (17) (2016) 5603–5614, https://doi.org/10.1021/jacs.6b0033210.1021/jacs.6b00332.s001.
[14] N. Eliaz, E. Gileadi, Physical Electrochemmistry : Fundamentals, Techniques, and Applications, second ed., Wiley-VCH, 2018.
[15] D.S. Hall, D.J. Lockwood, C. Bock, B.R. MacDougall, Nickel hydroxides and related materials: a review of their structures, synthesis and properties, Proc. Math. Phys. Eng. Sci. 471 (2174) (2015) 20140792, https://doi.org/10.1098/rspa.2014.0792.
[16] Y.Q. Gao, X.Y. Liu, G.W. Yang, Amorphous mixed-metal hydroxide nanostructures for advanced water oxidation catalysts, Nanoscale 8 (9) (2016) 5015–5023, https://doi.org/10.1039/C5NR08989A.
[17] L. Kuai, J. Geng, C. Chen, E. Kan, Y. Liu, Q. Wang, B. Geng, A Reliable Aerosol-Spray-Assisted Approach to Produce and Optimize Amorphous Metal Oxide Catalysts for Electrochemical Water Splitting, Angew. Chemie Int. Ed. 53 (29) (2014) 7547–7551, https://doi.org/10.1002/anie.201404208.
[18] F. Dionigi, P. Strasser, NiFe-Based (Oxy)hydroxide Catalysts for Oxygen Evolution Reaction in Non-Acidic Electrolytes, Adv. Energy Mater. 6 (23) (2016) 1600621, https://doi.org/10.1002/aenm.201600621.
[19] L. Trotochaud, S.L. Young, J.K. Ranney, S.W. Boettcher, Nickel-Iron Oxyhydroxide Oxygen-Evolution Electrocatalysts: The Role of Intentional and Incidental Iron Incorporation, J. Am. Chem. Soc. 136 (18) (2014) 6744–6753, https://doi.org/10.1021/ja502379c.
[20] Y. Xu, Y. Hao, G. Zhang, Z. Lu, S. Han, Y. Li, X. Sun, Room-temperature synthetic NiFe layered double hydroxide with different anions intercalation as an excellent oxygen evolution catalyst, RSC Adv. 5 (68) (2015) 55131–55135, https://doi.org/10.1039/C5RA05558J.
[21] X. Xiong, Z. Cai, D. Zhou, G. Zhang, Q. Zhang, Y. Jia, X. Duan, Q. Xie, S. Lai, T. Xie, Y. Li, X. Sun, X. Duan, A highly-efficient oxygen evolution electrode based on defective nickel-iron layered double hydroxide, Sci. China Mater. 61 (7) (2018) 939–947, https://doi.org/10.1007/s40843-017-9214-9.
[22] S. Jung, C.C.L. McCrory, I.M. Ferrer, J.C. Peters, T.F. Jaramillo, Benchmarking nanoparticulate metal oxide electrocatalysts for the alkaline water oxidation reaction, J. Mater. Chem. A 4 (8) (2016) 3068–3076, https://doi.org/10.1039/C5TA07586F.
[23] C.C.L. McCrory, S. Jung, J.C. Peters, T.F. Jaramillo, Benchmarking Heterogeneous Electrocatalysts for the Oxygen Evolution Reaction, J. Am. Chem. Soc. 135 (45) (2013) 16977–16987, https://doi.org/10.1021/ja407115p.
[24] M. del Arco, P. Malet, R. Trujillano, V. Rives, Synthesis and Characterization of Hydrotalcites Containing Ni(II) and Fe(III) and Their Calcination Products, Chem. Mater. 11 (3) (1999) 624–633, https://doi.org/10.1021/cm9804923.
[25] B. Lui, M. Zhang, Y. Wang, Z. Chen, K. Yan, Facile synthesis of defect-rich ultrathin NiCo-LDHs, NiMn-LDHs and NiCoMn-LDHs nanosheets on Ni foam

for enhanced oxygen evolution reaction performance, J. Alloys Comp. 852 (2021) 156949 (1 of 7). Doi: 10.1016/j.jallcom.2020.156949
[26] F. Cavani, F. Trifirò, A. Vaccari, Hydrotalcite-type anionic clays: Preparation, properties and applications, Catal. Today 11 (2) (1991) 173–301, https://doi.org/10.1016/0920-5861(91)80068-K.
[27] V. Rives, Layered Double Hydroxides: Present and Future, Nova Publishers, 2001.
[28] D.G. Evans, R.C.T. Slade, Structural Aspects of Layered Double Hydroxides. In: Duan X., Evans D.G. (eds) Layered Double Hydroxides. Structure and Bonding, vol 119. Springer, Berlin, Heidelberg. Doi: 10.1007/430_005
[29] M. Instruments, Zetasizer Nano Series Tech. Note. MRK654-01, 2010.
[30] C. Gomes, Z. Mir, R. Sampaio, A. Bastos, J. Tedim, F. Maia, C. Rocha, M. Ferreira, Use of ZnAl-Layered Double Hydroxide (LDH) to Extend the Service Life of Reinforced Concrete, Materials 13 (2020) 1769, https://doi.org/10.3390/ma13071769.
[31] R.D. Shannon, Revised effective ionic radii and systematic studies of interatomic distances in halides and chalcogenides, Acta Crystallogr. Sect. A 32 (5) (1976) 751–767, https://doi.org/10.1107/S0567739476001551.
[32] F.B.D. Saiah, B.-L. Su, N. Bettahar, Nickel-iron layered double hydroxide (LDH): textural properties upon hydrothermal treatments and application on dye sorption, J. Hazard. Mater. 165 (1-3) (2009) 206–217, https://doi.org/10.1016/j.jhazmat.2008.09.125.
[33] R. Gao, H. Zhang, D. Yan, Iron diselenide nanoplatelets: Stable and efficient water-electrolysis catalysts, Nano Energy 31 (2017) 90–95, https://doi.org/10.1016/j.nanoen.2016.11.021.
[34] L. Yao, N. Zhang, Y. Wang, Y. Ni, D. Yan, C. Hu, Facile formation of 2D Co2P@Co3O4 microsheets through in-situ toptactic conversion and surface corrosion: Bifunctional electrocatalysts towards overall water splitting, J. Power Sources 374 (2018) 142–148, https://doi.org/10.1016/j.jpowsour.2017.11.028.
[35] M. Arif, G. Yasin, M. Shakeel, M.A. Mushtaq, W. Ye, X. Fang, S. Ji, D. Yan, Highly active sites of NiVB nanoparticles dispersed onto graphene nanosheets towards efficient and pH-universal overall water splitting, J. Energy Chem. 58 (2021) 237–246, https://doi.org/10.1016/j.jechem.2020.10.014.